Nanoscale

Accepted Manuscript

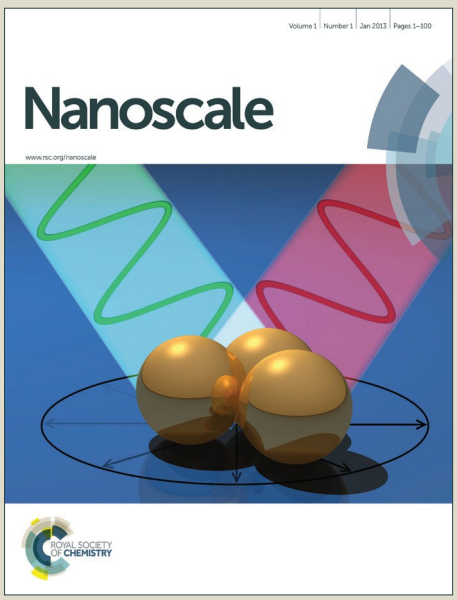

ROYAL SOCIETY OF CHEMISTRY

www.rsc.org/nanoscale

Cite this: DOI: 10.1039/c0xx00000x

www.rsc.org/xxxxxx

ARTICLE TYPE

In situ fabrication of a perfect Pd/ZnO@ZIF-8 core-shell microsphere as an efficient catalyst by a ZnO support-induced ZIF-8 growth strategy

Lu Lin,[a] Tong Zhang,[a] Haiou Liu,[a] Jieshan Qiu[a] and Xiongfu Zhang*[a]

Received (in XXX, XXX) Xth XXXXXXXXX 20XX, Accepted Xth XXXXXXXXX 20XX

DOI: 10.1039/b000000x

Controllable encapsulation of nanoparticles with metal organic frameworks (MOFs) has been an efficient way to impart the unique chemical and physical properties of the nanoparticles to metal organic frameworks and create new types of multifunctional MOF core-shell materials with enhanced properties. Here, a novel ZnO support-induced encapsulation strategy was reported to efficiently fabricate a Pd/ZnO@ZIF-8 core-shell catalyst with Pd/ZnO as the core and ZIF-8 as the shell. The novel synthesis procedure involves first loading Pd nanoparticles onto the surface of ZnO microsphere to form a Pd/ZnO core and then coating the core with a layer of defect-free ZIF-8 shell via ZnO-induced in-situ ZIF-8 growth to obtain the Pd/ZnO@ZIF-8 core-shell catalyst. It is crucial that ZIF-8 was in situ transformed from ZnO core in ethanol solution only containing 2-methylimidazole under mild conditions. This strategy allowed for the growth of ZIF-8 right on the surface of Pd/ZnO via the reaction between ZnO and 2-methylimidazole ligand, and thus avoided the random deposition of ZIF-8 crystals on the Pd/ZnO core in the case of conventional ZIF-8 synthesis solution. Furthermore, ethanol as the solvent also favored achieving the well-defined Pd/ZnO@ZIF-8 structure, since the ethanol solution of 2-methylimidazole was able to keep the balance between ZnO dissolution and ZIF-8 formation. The as-prepared Pd/ZnO@ZIF-8 core-shell microsphere as efficient catalyst displayed excellent performance in term of size-selectivity, stability and anti-poisoning in the liquid hydrogenations of alkenes.

1. Introduction

Metal organic frameworks (MOFs) are a class of newly-presented porous materials formed by assembling inorganic ions or clusters with organic ligands in suitable solvent. Compared with traditional porous materials, MOFs possess superiorities of ultrahigh porosity, enormous specific surface area, and tuneable structure,[1] which creates potential for applications on gas storage,[2] separation,[3] chemical sensor,[4] drug delivery[5] and catalysis.[6] Recently, it has come to attention that the controllable integration of functional components with MOFs has been used to manufacture core-shell nano- or micro-particle@MOFs materials.[7] This kind of material not only can retain the active properties of the particles and the molecular sieve function of MOFs but also can enhance the stability of the cores with small size and high surface energy by restricting them from aggregating and migrating.[8] In addition, some unique physical and chemical properties are likely to derive from the synergistic effect[8a] between the particles and MOFs.[8b] So far, the reported approaches to obtain MOFs coated core-shell structures have been summarized into two classes:[9] (a) post-synthesis incorporation of nanoparticles into as-prepared MOFs, (b) in-situ encapsulation of pre-synthesized nanoparticles with MOFs. When the former approach is attempted, the implementation of core-shell structure typically encounters challenge in the formation of nanoparticles into the cave of MOFs and suffers from the problem of the generation of particles on the surface of as-prepared MOFs, while the latter one constitutes a simple to fulfill strategy for circumventing this setbacks.[10]

ZIF-8, constructed by copolymerization of Zn (II) with 2-methylimidazolate, has become one of the most widely studied MOFs in fabricating core-shell materials by in-situ encapsulation due to their permanent porosity, high thermal stability and remarkable chemical resistance to boiling alkaline water and organic solvents.[11] Lu and co-workers[12] imparted a series of functional PVP-capped cores to a ZIF-8 material by controlled nanoparticle encapsulation, in which PVP benefited the adsorption of nanoparticles onto the continuously forming surfaces of the growing MOF crystals. Fu et al.[13] fabricated ZIF-8@SiO_2 core-shell microspheres as the stationary phase for liquid chromatography through modifying silica spheres with carboxylate. Our group[14] synthesized Pd/ZSM-5@ZIF-8 and Pd/SiO_2@ZIF-8 core-shell catalysts, which exhibited size-selectivity for hydrogenations of alkenes by electrostatic induction. It has been clear that the ZIF-8 shell over the core-shell material contributed to their high performance in wide-ranging applications. However, some special functional groups are needed in the above-mentioned approaches to achieve a layer of perfect ZIF-8 membrane/film. It is still challenging to develop a facile method to obtain well-defined and high-performance ZIF-8 coated core-shell materials. In term of shell growth of traditional methods, mass ZIF-8 crystals formed in the bulk synthesis solution are prone to pile up on the core and result in a defective ZIF-8 shell. Therefore, there is still lack of some artful strategies in the nucleation and growth of ZIF-8 right on the surface of the core.

In the present study, we developed a simple and efficient ZnO support-induced in situ encapsulation strategy to fabricate Pd/ZnO@ZIF-8 core-shell catalysts as shown in Scheme 1. In this strategy, ZnO was selected as a support and played

multifunctional roles. Firstly, ZnO is widely used as a catalyst support in heterogeneous catalysis[15] and able to facilitate the uniform dispersion of PdNPs to obtain a high-performance core-shell catalyst. Secondly, ZnO contains the same metal zinc as ZIF-8, thus can produce nucleation and growth sites right on its surface by providing Zn^{2+} source for the growth of ZIF-8 shell in the solution only containing 2-methylimidazole. This strategy could avoid the aforementioned issues as for traditional ZIF-8 synthesis solution and favor the encapsulation of the core with a layer of high-quality ZIF-8 shell. Furthermore, ethanol as the solvent of 2-methylimidazole solution also facilitated the fabrication of well-defined core-shell catalysts by equilibrating ZnO dissolution and ZIF-8 growth. The resulted Pd/ZnO@ZIF-8 core-shell catalyst performed very well as for activity, shape-selectivity and anti-inactivation in the hydrogenations of alkenes with different sizes.

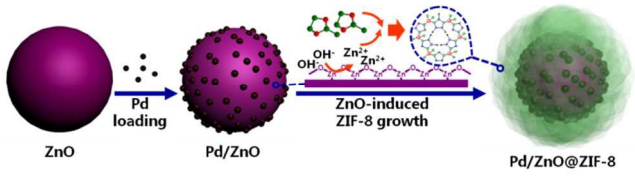

Scheme 1. Schematic illustration of Pd/ZnO@ZIF-8.

2. Experimental Section

2.1. Materials and Chemicals.

Ethanol (99.7%), methanol (99.5%), ethylacetate (99.5%), diethylene glycol (99%), zinc acetate dihydrate (99%), chlorinehydride (37%), benzothiazole (96%) and cyclohexene (99%) were purchased from Sinopharm Chemical Reagents Co., Ltd. Polyvinylpyrrolidone (PVP, Mw ≈ 40000) and 2-methylimidazolate (99%) were purchased from Sigma Adrich Chemical Co., Ltd. (Shanghai, China). Cyclooctene (95%) and 1-hexene (99%) were purchased from Aladdin Chemical Co., Ltd. $PdCl_2$ was obtained from Shanghai Jiuling Chemical Co., Ltd. Tert-Dodecylmercaptan (97%) was purchased from Alfar Aesar Chemical Co., Ltd. Deionized water was prepared in the laboratory.

2.2. Preparation of Pd/ZnO@ZIF-8 Core-Shell Catalysts

The preparation route is indicated in the above Scheme 1, PdNPs were first loaded on ZnO spheres to form Pd/ZnO as cores. Then the Pd/ZnO cores were placed in a 2-methylimidazole ligand solution containing no any zinc source for ZIF-8 shell growth to form Pd/ZnO@ZIF-8 core-shell spheres. The detail is as follows:

Synthesis of ZnO Spheres

ZnO spheres with an average diameter of 300 nm were synthesized by homogeneous precipitation. In a typical process, zinc acetate dihydrate (1.098 g, 0.005 mol) was dissolved in diethylene glycol (50 mL). And then the mixture was heated to 433 K and kept stirring for 2 h at this temperature. Finally the reaction vessel was cooled to room temperature. The ZnO spheres were recovered by centrifugation and washed three times with ethanol.

Synthesis of Pd Nanoparticles

Pd nanoparticles of around 5 nm were prepared by the ethanol reduction of H_2PdCl_4. Typically, 2 mM H_2PdCl_4 aqueous solution (15.0 mL), deionized water (21.0 mL), PVP (66.7 mg, 1.7 μmol) and 1 M HCl (0.8 mL) were mixed and heated. When the solution began to reflux, ethanol (14.0 mL) was added. The solution then continued to reflux for 3 h to obtain a dark brown suspension of PVP-stabilized Pd NPs.

Preparation of Pd/ZnO Catalysts

In a typical synthesis, the as-prepared ZnO (0.08 g, 0.98 mmol) spheres were mixed with the suspension of PVP stabilized Pd NPs (1.0 mL). The mixture was stirred at room temperature for 15 h. The Pd/ZnO catalyst was collected by centrifugation and rinsed with ethanol several times. The Pd loading of the Pd/ZnO catalyst determined by inductively coupled plasma atomic emission spectroscopy (ICP-AES) was 0.69 wt%.

Formation of Pd/ZnO@ZIF-8 Core-Shell Catalysts

First of all, the as-prepared Pd/ZnO (0.08 g) particles were dispersed in ethanol (4.0 mL) and 2-methylimidazole (0.8 g, 9.8 mmol) was dissolved in ethanol (16 mL). These two solutions were then mixed for ZIF-8 shell growth. The mixture was held under vigorous stirring at 323 K for 2 h and then collected by centrifugation and washed with ethanol for several times to obtain the core-shell product. The Pd loading of the Pd/ZnO@ZIF-8 determined by ICP-AES was 0.48 wt%.

Formation of Pd/SiO_2@ZIF-8 Core-Shell Catalysts:

For comparison, the Pd/SiO_2@ZIF-8 core-shell catalysts were also synthesized according to the traditional method we reported previously[14] The Pd loading of Pd/SiO_2@ZIF-8 determined by ICP-AES was 0.08 wt%.

2.3. Characterization of Materials.

Powder X-ray diffraction (PXRD) patterns were collected on a D/max-2400 diffractometer with a Cu target (40 kV, 100 mA) from 5° to 80° at a scanning rate of 10°/min. The morphology of each sample was observed by field-emission scanning electron microscopy (FE-SEM) on a Nova NanoSEM 450 microscope and by transmission electron microscopy (TEM) on a Tecnai F30 microscope at 300 kV. Nitrogen sorption isotherms were measured using an AUTOSORB-1-MP analyzer at 77 K. Infrared spectras of the samples were recorded on a Bruker EQUINOX55 Fourier transform (FT) IR spectrometer in the spectral range of 4000-400 cm^{-1} using the potassium bromide disk method. Thermogravimetric analysis (TGA) was carried out in air using a TG/SDTA 851E instrument at the temperature from 298 to 873 K with a ramp of 10 $K \cdot min^{-1}$. Elemental analysis was performed by ICP-AES using an Optima 179 2000DV spectrometer.

2.4. Catalytic Hydrogenations of Alkenes

Hydrogenations of alkenes (1-hexene, cyclohexene, and cyclooctene) were carried out in ethyl acetate solution in a static hydrogen atmosphere. In each experiment, the catalyst (0.04 g) was placed in a reactor, and the air in the reactor was expelled by flushing several times with hydrogen. Then, ethyl acetate (5.0 mL) and 1-hexene (2.43 mL) were added to the reactor. After the reactor had been flushed one more time with hydrogen, the reaction was allowed to proceed under hydrogen atmosphere (1 bar) at 308 K for 24 h. When the reaction was done, the sample was removed from the reactor and centrifuged, and the filtrate was analyzed using a gas chromatograph equipped with an HP-5

column and a flame ionization detector. The catalyst-to-substrate molar ratio was always kept at 1:10000. For recycling experiments, the used catalysts were separated by centrifugation and then washed thoroughly with ethyl acetate. For anti-poisoning test, the concentration of the toxic was 500 ppm.

3. Results and Discussion

3.1. Formation and Characterization of Pd/ZnO@ZIF-8 Core-Shell Catalysts.

Preparation and Structures of Pd/ZnO@ZIF-8 Microspheres: The synthetic process of Pd/ZnO@ZIF-8 catalysts is outlined in Scheme 1 and the results are shown in Figure 1 and 2. PVP capped Pd nanoparticles (Pd NPs) of about 5 nm (Figure 1a) were loaded on the ZnO microspheres of 400 nm (Figure 1b) in average to form Pd/ZnO supported catalysts. Due to the existence of hydrogen bond or ionic bond between the surface hydroxyl group of the ZnO and PVP,[16] the as-prepared Pd/ZnO catalysts were stable enough to prevent the Pd NPs from falling off during the subsequent formation process of ZIF-8 shell under mild conditions. Figure 1c and 1d are the TEM images of Pd/ZnO. Clearly, the Pd NPs showing as darker spots were dispersed on the surface of ZnO supports.

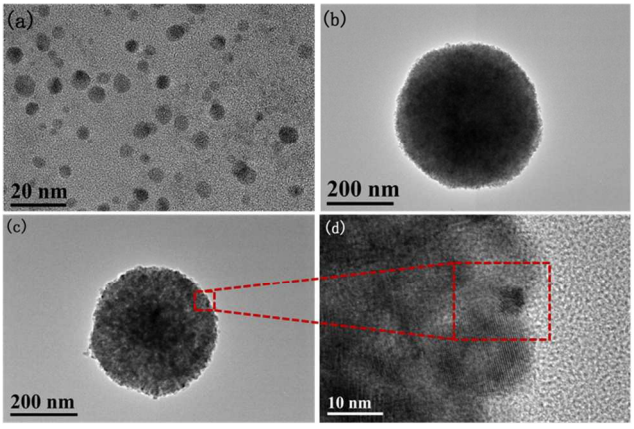

Figure 1. TEM images of (a) PdNPs, (b) ZnO, (C) and (d) Pd/ZnO

The formation of a layer of perfect ZIF-8 shell over a core was a vital step for the fabrication of a core-shell ZIF-8-based structure. Generally, the core had to be modified with some organic groups or ZIF-8 seeds to facilitate the formation of ZIF-8 over the core.[12-14, 17] In this study, the facile fabrication of high-quality core-shell Pd/ZnO@ZIF-8 catalysts was obtained by reacting 2-methylimidazole with Zn^{2+} produced by the ZnO core in ethanol solution of 2-methylimidazole at 323 K for 2 h. As shown in Figure 2a and 2b, the size of the microspheres became larger than that of the original Pd/ZnO core and the surface of Pd/ZnO core was closely packed with hexahedron ZIF-8 nanocrystals, showing that a layer of ZIF-8 shell grew well on the core. Figure 2c and 2d are typical TEM images of Pd/ZnO@ZIF-8. The average thickness of the outer ZIF-8 shell was about 95 nm and the diameter of the inner Pd/ZnO core was about 350 nm averagely. It also can be seen from the high-magnification TEM image (Fig. 2d) that many Pd NPs located on the surface of Pd/ZnO were firmly enwrapped with ZIF-8 shell after the treatment of Pd/ZnO with 2-methylimidazole solution.

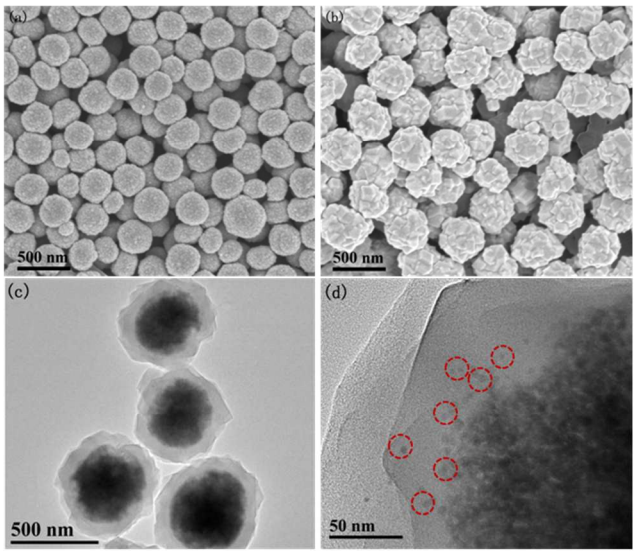

Figure 2. SEM images of (a) ZnO, (b) Pd/ZnO@ZIF-8 and (c, d) TEM images of Pd/ZnO@ZIF-8.

Remarkably, compared with those prepared by the conventional method which involved pre-treatment for the core and the subsequent shell growth in a ZIF-8 synthesis solution for two times, the ZIF-8 shell formed by ZnO induction was highly denser and more continuous (Figure 3). And as seen from the following reaction section, the core-shell catalysts also performed better in terms of shell integrity and selectivity (Table 1). It is because that in the case of coventional synthesis solution of ZIF-8 that contained enough metal ions and organic ligands, ZIF-8 nanoparticles formed in the bulk synthesis solution tended to deposit on the core, which seriously influenced the formation of a layer of perfect shell. Moreover, such ZIF-8 shell was also liable to peel off from the core due to weak adhesion between the shell and the core during its applications, resulting in the decay of the core-shell catalyst in some functional properties. On the contrary, ZnO, as the only Zn^{2+} souce, could provide growth sites for ZIF-8 and strictly limit the formation of ZIF-8 shell to the surface of Pd/ZnO core, resulting in well-defined and high-performance core-shell catalysts. Besides, this strategy can also produce more monodispersed core-shell composite by avoiding the second growth of ZIF-8 which aims to increase the compactness of the outer shell, since in the process of second growth, contiguous part of different Pd/SiO_2@ZIF-8 catalysts tended to be coated by newly-formed ZIF-8 shell, leading to aggregation and bulk crystallization.

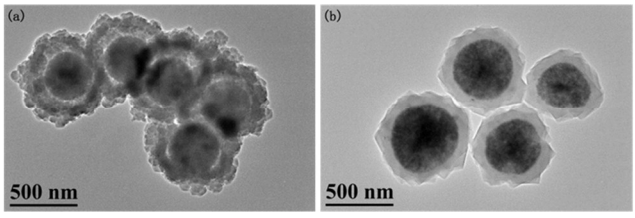

Figure 3. TEM images of (a) Pd/SiO_2@ZIF-8 synthesized by conventional method,[14] (b) Pd/ZnO@ZIF-8 achieved by this strategy.

Figure 4 shows some texture properties of the achieved Pd/ZnO@ZIF-8 structures. The XRD patterns of Pd/ZnO@ZIF-8 matched well with those of ZIF-8 and ZnO (Figure 4a). The

missed Pd characteristic peaks might be due to the small particle size of the Pd NPs and the low content of elemental Pd on the surface.[18] The characteristic peaks of ZIF-8 displayed in the IR spectrum of the Pd/ZnO@ZIF-8 in Figure 4c indicated the existence of ZIF-8 shell on the core-shell catalyst. The band at 421 cm^{-1} was assigned to the Zn-N stretch mode. The plane bending and stretching of imidazole ring were contributed to the bands in the spectral regions of 500-1350 cm^{-1} and 1350-1500 cm^{-1}, respectively. The C-N stretch mode was at 1584 cm^{-1} and peaks for the aromatic and aliphatic C-H stretch were expected at 2929 cm^{-1} and 3135 cm^{-1}.[19]

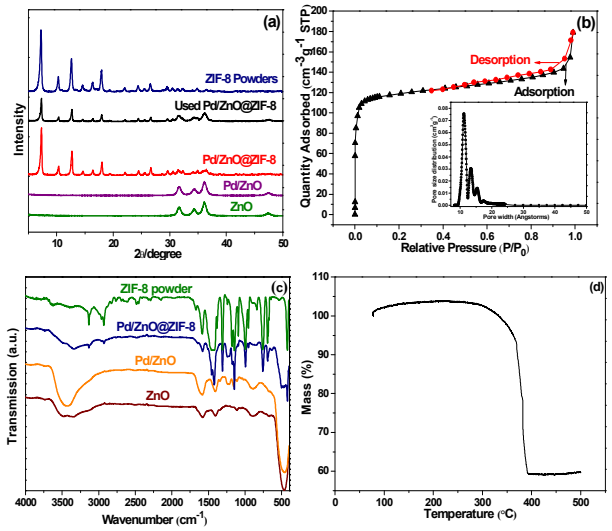

Figure 4. (a) XRD patterns of different samples. [Note: Used Pd/ZnO@ZIF-8 is the catalyst sample after being recycled in the reaction for four times.] (b) (inset: Corresponding pore-size distributions calculated by the Horvath–Kawazoe method) N_2 adsorption-desorption isotherm of Pd/ZnO@ZIF-8. (c) FT-IR spectra of different samples. (d) TGA curve of Pd/ZnO@ZIF-8.

The nitrogen sorption-desorption isotherms of the core-shell catalyst at 77 K showed a type I isotherm with steep increase in N_2 uptake at a low relative pressure (Fig. 4b), which confirmed the formation of microporous structure of ZIF-8 shell. The Brunauer-Emmett-Teller (BET) surface area and pore volume of the samples were 435.80 m^2g^{-1} and 0.28 cm^3g^{-1}, respectively, which were lower than those of pure ZIF-8. This could be due to the high contribution of the nonporous ZnO core to the mass of the core-shell catalyst. The thermogravimetic (TGA) analysis of Figure 4d demonstrated the good thermal stability of the core-shell catalyst with the decomposition temperature of which was about 593 K. The decrease in decomposition temperature of Pd/ZnO@ZIF-8 might come from the differences in the size of pure ZIF-8 and ZIF-8 shell.[20]

Formation Mechanism of Pd/ZnO@ZIF-8 Microspheres:

The formation process of the ZIF-8 shell over Pd/ZnO was investigated by TEM analysis (Figure 5) using the Pd/ZnO core of about 235 nm with time-dependent reaction in the ethanol solution of 2-methylimidazole at 323 K. At the time point of 2 minutes (Figure 5b), the smooth surface of Pd/ZnO became rougher and partly packed with ill-defined ZIF-8 nucleis of about 35 nm. After 2 h (Figure 5c), these ZIF-8 nanoparticles gradually became larger and intergrew better, forming a thin layer of ZIF-8 shell with average thickness of about 80 nm. Simultaneously, the shape of inner ZnO sphere became irregular with its size reducing to about 216 nm, which resulted in the Pd NPs encapsulated with ZIF-8 shell. After the reaction of 6 h (Figure 5d), the thickness of ZIF-8 shell increased to about 100 nm, while the size of the ZnO core also decreased to approximately 200 nm. For longer reaction time of 18 h (Figure 5e), no visible change in dimension was observed. Based on the above traced results, it was evident that as the time went on, the ZIF-8 shell grew thicker and thicker, while the ZnO core became smaller and smaller. A stable and perfect core-shell structured Pd/ZnO@ZIF-8 catalyst was formed with thicker and denser ZIF-8 shell firmly enwrapped around the smaller Pd/ZnO core.

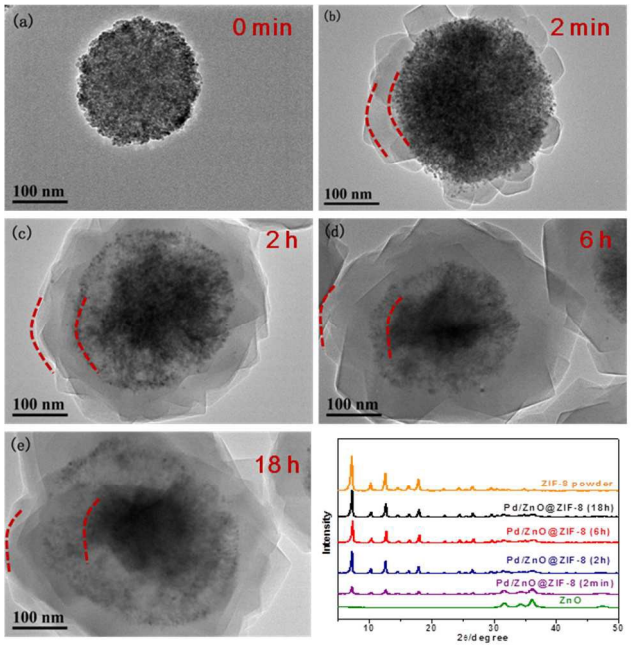

Figure 5. TEM images of (a) Pd/ZnO, (b-e) Pd/ZnO@ZIF-8 obtained after reaction for 2 min, 2h, 6h, and 18h, respectively; f) corresponding XRD patterns of Pd/ZnO@ZIF-8 as a function of reaction time.

The transformation of ZnO to ZIF-8 was also inferred from the XRD patterns (Figure 5f). For the sample reacted at 2 min, besides diffraction peaks of ZnO, several weak diffraction peaks agreed well with those of ZIF-8. As the reaction time proceeded, the ZIF-8-related peaks became stronger and stronger. These changes could be the attribution of the special growth mechanism of the ZIF-8 shell, coined "dissolution-recrystallization".[21] In fact, the ZnO core could serve as the nucleation, growth and anchoring sites of ZIF-8 shell by providing Zn^{2+} source for ZIF-8 formation in the ethanol solution of 2-methylimidazole. When the Pd/ZnO core was placed into the solution for shell growth, ZnO could be slightly dissolved and release Zn^{2+} ions on the interface of the solid because of the weak alkalinity of the solution (pH=8).[22] Then these free Zn^{2+} ions would rapidly react with 2-methylimidazole to form ZIF-8 structure right on the surface of the ZnO core. This process was crucial for the tight growth of ZIF-8 on a substrate. As the time went on, ZnO was constantly consumed and ZIF-8 was formed, thus resulting in the significant decrease in the size of the ZnO sphere and the increase in thickness of ZIF-8 shell. When the shell got thick enough, 2-methylimidazole in the solution and Zn^{2+} ions from the ZnO core

could hardly go through the ZIF-8 shell and contact with each other. As a result, the thickness of ZIF-8 shell was kept almost constant with further prolonging the time. Guessingly, Pd NPs might have leached into the solution during the process of ZnO dissolution, since they were dispersed on the surface of ZnO. In order to confirm whether the PdNPs was leaching during the synthesis of ZIF-8, the reacted compound after the shell growth was centrifuged and the supernate was recovered to test the catalytic activity in the hydrogenation of 1-hexene. The results showed that there was not any activity, which confirmed the absence of PdNPs in the liquid supernate and excluded the leaching of the PdNPs from the Pd/ZnO core during the formation of ZIF-8 shell. This should be the contribution of the hydrogen bond or ionic bond between the surface hydroxyl group of the ZnO and PVP,[16] together with the weak coordination interactions between pyrrolidone rings (C=O) of PVP and zinc atoms in ZIF nodes, and perhaps hydrophobic interactions between apolar groups of PVP and organic linkers.[12]

The rapid formation and growth of ZIF-8 on the interface of the core could help to encapsulate PdNPs with the shell as soon as possible and avoid Pd leaching as well. This mainly depended on the solvent used in 2-methylimidazole solution, which could change the pH value of the solution and then affect the balance between the dissolution of ZnO and formation of ZIF-8. In fact, it was found in our study that the solvent used in 2-methylimidazole solution played an important role in forming well-defined core-shell catalysts.

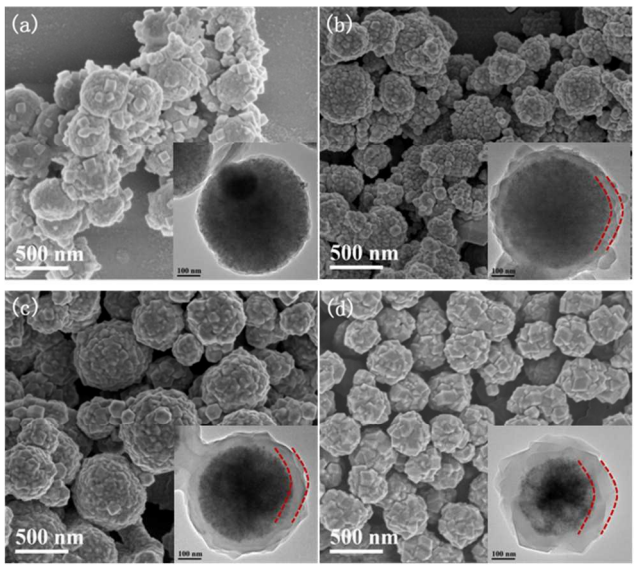

Figure 6. SEM images and TEM images (inset) of the products obtained with different ratios of H_2O to ethanol (volume to volume) at 323 K for 2h: (a) 1:0, (b) 3:1, (c) 1:3, (d) 0:1.

In this study, different amount of H_2O was added into the ethanol solution of 2-methylimidazole to investigate the effect of the ratios of water to ethanol on the formation of the Pd/ZnO@ZIF-8 core-shell structure. Figure 6 displays the morphology of Pd/ZnO@ZIF-8 with different amount of H_2O added into the solution. In the case of H_2O as the only solvent (Figure 6a), ZIF-8 crystals were partly packed on the core and no continuous shell was formed. This is because the dissolution of ZnO was faster than the growth of ZIF-8 due to the higher alkalinity (pH=9) in the water solution of 2-methylimidazole, thus leading to the formation of ZIF-8 mainly in the bulk solution rather than on the surface of the ZnO core. As the amount of ethanol increasing (Figure 6b and 6c), the ZIF-8 shell became thicker and more continuous and the freestanding ZIF-8 particles either on the core or in the bulk solution were less. For pure ethanol used as solvent (Figure 6d), a layer of perfect ZIF-8 shell tightly grew on the surface of Pd/ZnO with rare individual ZIF-8 particles. In comparison, ethanol as solvent in 2-methylimidazole solution greatly favored the growth of a ZIF-8 shell on the Pd/ZnO core to form a high-quality Pd/ZnO@ZIF-8 core-shell structure. This could be mainly attributed to the fact that rapid formation of ZIF-8 on the core matched well with the slow dissolution of ZnO in ethanol solution,[23] which could also avoid the formation of ZIF-8 crystals in the bulk solution and their free pileup on the core.

3.2 Catalytic Hydrogenation Performance of Pd/ZnO@ZIF-8 Core-shell Catalysts

ZIF-8 possesses a micro pore in diameter of 3.4 Å and allows for molecules smaller than 3.4 Å to pass through. Therefore, a well-defined Pd/ZnO@ZIF-8 core-shell catalyst could perform molecular-sieving capability with outer ZIF-8 shell as selective membrane. To confirm the shell integrality and its size selectivity, liquid hydrogenations of 1-hexene, cyclohexene and cyclooctene were employed as model reactions and the results were listed in Table 1, Table 2 and Figure 7a. For 1-hexene with the kinetic diameter of 1.7 Å, it is small enough to go through the ZIF-8 shell and gets in touch with PdNPs easily. Therefore, the core-shell catalyst showed high activity with the conversion of 100% in the hydrogenation of 1-hexene. Compared with the supported Pd/ZnO catalyst (Figure 7a), the core-shell catalysts gave a slower reaction rate possibly because of the steric hindrance caused by the ZIF-8 shell. When it came to sterically more demanding cyclooctene (5.4 Å), the catalyst performed no conversion of it. Thus, non-existence of PdNPs on the outer surface of ZIF-8 shell was also confirmed.

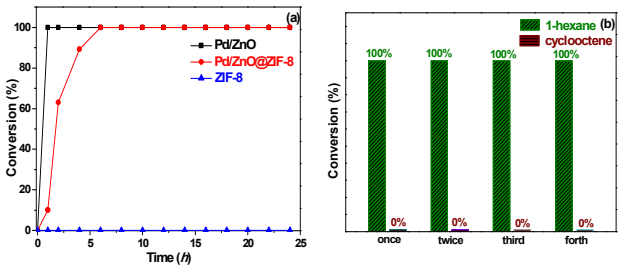

Figure 7. (a) Kinetic curves or the hydrogenation of 1-hexene over different catalysts, (b) recycling experiments of the Pd/ZnO@ZIF-8 for alkene hydrogenations.

It should be noted that cyclohexene (4.2 Å) could still pass through ZIF-8 shell and got a conversion of about 13.9%, though its size is larger than that of the pore diameter of ZIF-8. This result accords with reported literature and should be ascribed to the framework flexibility of ZIF-8.[24e] Several evidences show that the 2-methyimidazole ligands of ZIF-8 tend to rotate under pressure or introduction of guest molecules at room temperature. As a result, the effective aperture size of ZIF-8 is extended to about 4.2 Å.[24] In the control experiments, ZIF-8 itself displayed

no propensity to catalyze these reactions (Table 1). The Pd/ZnO as catalyst performed high activities in the hydrogenations of 1-hexene (100%) and cyclohexene (100%) and relatively low conversion of cyclooctene (8.9%). The Pd/SiO_2@ZIF-8 core-shell catalysts reported by our group[14] were also synthesized by pretreatment of core with polyelectrolyte and subsequent shell growth in a ZIF-8 synthesis solution. Although with no activity for cyclooctene, Pd/SiO_2@ZIF-8 still showed a much higher conversion of cyclohexene (29.2%) compared with Pd/ZnO@ZIF-8. This implied that the ZIF-8 shell of the Pd/SiO_2@ZIF-8 might have some defects. It is clearly seen from the TEM images (Figure. 3) of the core-shell catalysts obtained by two different preparation methods that the ZIF-8 shell by this novel method is denser and more tightly combined with the core than that by the traditional one. These results demonstrated the integrity and selectivity of ZIF-8 shell synthesized in ZnO-induced strategies were better than that generated by conventional methods which involved pre-treatment for the core and subsequent growth in a ZIF-8 synthesis solution.

Table 1. Size-selective hydrogenations of different single-component reactants over different catalysts[a]

Catalysis	Conversion (100%)		
	1-hexene	Cyclohexene	Cyclooctene
ZIF-8	0	0	0
Pd/ZnO	100	100	8.9
Pd/SiO_2@ZIF-8[b]	100	29.2	0
Pd/ZnO@ZIF-8	100	13.9	0

[a]Reaction performed at 308 K for 24 h under H_2 (1 bar, balloon) in ethyl acetate (5.0 mL) with a catalyst-to-substrate molar ratio of 1:10000.
[b]Pd/SiO_2@ZIF-8 was synthesized by conventional method.[14]

Table 2. Size-selective hydrogenations of multicomponent reactants over Pd/ZnO@ZIF-8 catalysts[a]

Reactant Component	Conversion (100%)		
	1-hexene	Cyclohexene	Cyclooctene
Equimolar three-component mixture	100	0.2	0
Equimolar two-component mixture	100	9.5	—
Equimolar two-component mixture	—	0.4	0

[a]Reaction performed at 308 K for 24 h under H_2 (1 bar, balloon) in ethyl acetate (5.0 mL) with a catalyst-to-substrate molar ratio of 1:10000.

In terms of the hydrogenation of equimolar three-component mixture, our core-shell catalyst displayed even better size-selectivity. As shown in Table 2., the Pd/ZnO@ZIF-8 catalyst showed a conversion of 100% for 1-hexene and no activity for cyclooctene. Notably, the conversion of cyclohexene over it was only 0.2%. By comparing the selectivity of two kinds of equimolar two-component mixtures, it is clear that the conversion of cyclohexene was largely influenced by cyclooctene. Therefore, this higher selectivity might be mainly attributed to the competitive adsorption and mutual influence between cyclohexene and cyclooctene during the reaction.

The stability of a catalyst is also an important factor to evaluate its catalytic performance in liquid heterogeneous catalysis. In our studies, the examination of the catalyst stability was not only focused on the anti-leaching of Pd active sites but also on the selectivity of ZIF-8 shell. To test whether PdNPs leached from Pd/ZnO@ZIF-8 to liquid system during the reaction, the solid catalyst was separated from the reaction solution by centrifugation after reacting for 72 h and the liquid supernatant was applied to catalyze the hydrogenation of 1-hexene again. No extra reaction product was detected after the reaction for 48 h, while approximately 6.54% of 1-hexene converted to 1-hexane in the case of Pd/ZnO. The anti-leaching property of the core-shell catalyst could be explained by the existence of perfect ZIF-8 shell which prevented the PdNPs from leaching during the reaction.

The stability of ZIF-8 shell in term of size-selectivity was examined in the hydrogenations of hexene and cyclooctene as shown in Figure 7b. The Pd/ZnO@ZIF-8 catalyst kept both high activity of 100% for 1-hexene and excellent selectivity for cyclooctene during the process of all four recycles. No activity for the hydrogenation of cyclooctene was observed and the PXRD pattern (used Pd/ZnO@ZIF-8 of Figure 4a) of the core-shell catalyst remained unchanged after four cycles, confirming that the crystalline structure and integrity of the ZIF-8 shell were still kept very well during the recycling.

Apart from the leaching of active sites, the existence of sulfur-based impurities is also an important reason for catalyst deactivation.[25] Generally, sulfur poisoning is resulted from the strong bond between sulfur and metal sites and the formation of stable but unwanted metal sulfides.[26] Herein, the encapsulation of PdNPs with microporous ZIF-8 shell could, to some extent, prevent the combination of sulfur poison and Pd sites.

Table 3 listed the reaction results of the liquid hydrogenation of 1-hexene containing a certain amount (500ppm) of sulfides over Pd/ZnO and Pd/ZnO@ZIF-8. It was clear that for relatively smaller sulfide molecules, such as benzothiazole and tert-dodecanethiol, the core-shell catalyst could show high conversion of about 94.8% and 73.7%, respectively, while the Pd/ZnO catalyst without ZIF-8 shell gave a yield of less than 6% for two sulfides. This indicated that outer ZIF-8 shell even with thickness of about 100 nm was compact enough to protect the PdNPs from most small sulfur poisons. Therefore, the achieved core-shell catalyst possesses anti-poisoning superiority compared with the supported Pd/ZnO catalyst.

Table 3. Comparison of the sulfur-resistant properties of Pd/ZnO and Pd/ZnO@ZIF-8[a]

Catalysis	Conversion (%)	
	Benzothiazole	Tert-dodecanethiol
Pd/ZnO	5.5	5.3
Pd/ZnO@ZIF-8	94.8	73.7

[a]Reaction performed at 308 K for 24 h under H_2 (1 bar, balloon) in ethyl acetate (5.0 mL) which contains 500ppm of poisons with a catalyst-to-substrate molar ratio of 1:10000.

Conclusions

In conclusion, the facile and efficient fabrication of a new-type perfect Pd/ZnO@ZIF-8 core-shell catalyst was successfully developed via a "support-induced encapsulation" strategy. ZnO not only serves as the support for the trapping of PdNPs to form a Pd/ZnO core, but also provides the nucleation, growth and

anchoring sites for the growth of ZIF-8 shell by producing Zn^{2+} source right on the ZnO surface for the formation of ZIF-8 structure. This method eliminates the conventional synthesis step in ZIF-8 synthesis solution to avoid random deposition of ZIF-8 crystals formed from the synthesis solution on the cores, and facilitates the formation of a high-quality Pd/ZnO@ZIF-8 core-shell catalyst. The selection of ethanol as solvent in 2-methylimidazole solution is crucial to the growth of a perfect ZIF-8 shell over the Pd/ZnO core, as the amount of Zn^{2+} ions released from ZnO dissolution in ethanol solution of 2-methylimidazole can match very well with that needed for the formation of ZIF-8. The obtained core-shell catalyst demonstrated high selectivity for small molecules and performed well in term of catalyst stability and anti-poisoning in the liquid hydrogenation of alkenes. This metal oxide support-induced encapsulation of nanoparticles strategy provides possibility for the synthesis of other kinds of NPs@MOFs structures and finds opportunities in the field of catalysis and selective adsorption.

Acknowledgements

The authors would like to thank the financial support by the National Natural Science Foundation of China (No. 21173030, 21076030, 21476039).

Notes and references

[a]*State Key Laboratory of Fine Chemicals, School of Chemical Engineering, Dalian University of Technology, Dalian, P. R. China, Fax/Tel：+86-411-84986155, E-mail: xfzhang@dlut.edu.cn (X. F. Zhang)*

1 H. C. Zhou, J. R. Long, O. M. Yaghi, *Chem. Rev.*, 2012, **112**, 673-674.

2 a) L. J. Murray, M. Dincă, J. R. Long, *Chem. Soc. Rev.*, 2009, **38**, 1294-1314. b) N. L. Rosi, J. Eckert, M. Eddaoudi, D. T. Vodak, J. Kim, M. O'Keeffe, O. M. Yaghi. *Science*, 2003, **300**, 1127-1129. c) J. L. C. Rowsell, O. M. Yaghi, *Angew. Chem. Int. Ed.*, 2005, **44**, 4670-4679.

3 a) J. R. Li, R. J. Kuppler, H. C. Zhou, *Chem. Soc. Rev.*, 2009, **38**, 1477-1504. b) J. R. Li, J. Sculley, H. C. Zhou, *Chem. Rev.*, 2011, **112**, 869-932.

4 a) Z. Hu, B. J. Deibert, J. Li, *Chem. Soc. Rev.*, 2014, **43**, 5815-5840. b) L. E. Kreno, K. Leong, O. K. Farha, M. Allendorf, R. P. V. Duyne, J. T. Hupp, *Chem. Rev.*, 2012, **112**, 1105-1125. c) J. H. Lee, J. Justyn, H. J. Jong, *Nanoscale*, 2013, **5**, 8533-8540.

5 a) M. L. K. Taylor-Pashow, J. D. Rocca, Z. Xie, S. Tran, W. B. Lin, *J. Am. Chem. Soc.*, 2009, **131**, 14261-14263. b) P. Horcajada1, T. Chalati, C. Serre, B. Gillet, C. Sebrie, T. Baati, J. F. Eubank, D. Heurtaux, P. Clayette, C. Kreuz, J. Chang, Y. K. Hwang, V. Marsaud, P. Bories, L. Cynober, S. Gil, G. Férey, P. Couvreur, R. Gref, *Nature Chem.*, 2010, **9**, 172-178. c) P. Horcajada, C. Serre, M. Vallet-Regí, M. Sebban, F. Taulelle, G. Férey, *Angew. Chem. Int. Ed.*, 2006, **45**, 5974-5978.

6 a) D. Farrusseng, S. Aguado, C. Pinel, *Angew. Chem. Int. Ed.*, 2009, **48**, 7502-7513. b) M. Yoon, R. Srirambalaji, K. Kim, *Chem. Rev.*, 2011, **112**, 1196-1231. c) L. Shen, W. Wu, R. Liang, R. Lin, L. Wu, *Nanoscale*, 2013, **5**, 9374-9382. d) K. Fei, L. G. Qiu, J. F. Zhu, *Nanoscale*, 2014, **6**, 1596-1601

7 a) M. Meilikhov, K. Yusenko, D. Esken, S. Turner, G. V. Tendeloo, R. A. Fischer, *Eur. J. Inorg. Chem.*, 2010, **24**, 3701-3714. b) A. Dhakshinamoorthy, H. Garcia, *Chem. Soc. Rev.*, 2012, **41**, 5262-5284.

8 (a) G. H. Yang, N. Tsubaki, J. Shamoto, Y. Yoneyama, Y. Zhang, *J. Am. Chem. Soc.*, 2010, **132**, 8129-8136. (b) H. R. Moon, D. -W. Lim, M. P. Suh, *Chem. Soc. Rev.*, 2013, **42**, 1807-1824.

9 Y. L. Liu, Z. Y. Tang, *Adv. Mater.*, 2013, **25**, 5819-5825.

10 a) K. Na, K. M. Choi, O. M. Yaghi, G. A. Somorjai, *Nano lett.*, 2014, **14**, 5979. b) W. N. Zhang, G. Lu, C. L. Cui, Y. Y. Liu, S. Z. Li, W. J. Yan, C. Xing, Y. R. Chi, Y. H. Yang, F. W. Huo, *Adv. Mater.*, 2014, **26**, 4056-4060.

11 a) K. S. Park, Z. Ni, A. P. Côté, J. Y. Choi, R. Huang, F. J. Uribe-Romo, H. K. Chae, M. O'Keeffe, O. M. Yaghi, *Proc. Natl. Acad. Sci. USA.*, 2006, **103**, 10186-10191. b) R. B. Wu, D. P. Wang, J. Y. Han, H. Liu, K. Zhou, Y. Z. Huang, R. Xu, J. Wei, X. D. Chen, Z. Chen, *Nanoscale*, 2015, **7**, 965-974.

12 G. Lu, S. Z. Li, Z. Guo, O. K. Farha, B. G. Hauser, X. Y. Qi, Y. Wang, X. Wang, S. Y. Han, X. G. Liu, J. S. DuChene, H. Zhang, Q. C. Zhang, X. D. Chen, J. Ma, S. C. J. Loo, W. D. Wei, Y. Yang, J. T. Hupp, F. W. Huo, *Nature Chem.*, 2012, **4**, 310-316.

13 Y. Y. Fu, C. X. Yang, X. P. Yan, *Chem. Eur. J.*, 2013, **19**, 13484-13491.

14 a) T. Zhang, X. F. Zhang, X. J. Yan, L. Lin, H. O. Liu, J. S. Qiu, K. L. Yeung, *Catal. Today*, 2013, **236**, 36-40. b) T. Zhang, B. Li, X. F. Zhang, J. S. Qiu, W. Han, K. L. Yeung, *Microporous Mesoporous Mater.*, 2014, **197**, 324-330. c) L. Lin, T. Zhang, X. F. Zhang, H. O. Liu, K. L. Yeung, J. S. Qiu. *Ind. Eng. Chem. Res.*, 2014, **53**, 10906-10913.

15 J. Strunk, K. Kähler, X. Xia, M. Muhler, *Surf. Sci.*, 2009, **603**, 1776-1783.

16 R. K. Iler, *The chemistry of silica: solubility, polymerization, colloid and surface properties, and biochemistry*. Wiley Interscience, New York, 1979.

17 a) S. Sorribas, B. Zornoza, C. Téllez, J. Coronas, *Chem. Commun.*, 2012, **48**, 9388-9390. b) H. Ren, L. Y. Zhang, J. P. An, T. T. Wang, L. Li, X. Y. Si, L. He, X. T. Wu, C. G. Wang, Z. M. Su, *Chem. Commun.*, 2014, **50**, 1000-1002.

18 Y. Y. Pan, D. Y. Ma, H. M. Liu, H. Wu, D. H. He, Y. W. Li, *J. Mater. Chem.*, 2012, **22**, 10834-10839.

19 Y. Hu, S. Kazemian, S. Rohani, Y. N. Huang, Y. Song, *Chem. Commun.*, 2011, **47**, 12694-12696.

20 Y. C. Pan, Y. Y. Liu, G. F. Zeng, L. Zhao, Z. P. Lai, *Chem. Commun.*, 2011, **47**, 2071-2073.

21 a) W. W. Zhan, Q. Kuang, J. Z. Zhou, X. J. Kong, Z. X. Xie, L. S. Zheng, *J. Am. Chem. Soc.*, 2013, **135**, 1926-1933. b) L. H. Lee, N. Janssens, S. P. Sree, C. Wiktor, E. Gobechiya, R. A. Fischer, C. E. A. Kirschhock, J. A. Martens, *Nanoscale*, 2014, **6**, 2056-2060.

22 Q. Kuang, T. Xu, Z. X. Xie, S. C. Lin, R. B. Huang, L. S. Zheng, *J. Mater. Chem.*, 2009, **19**, 1019-1023.

23 E. L. Bustamante, J. L. Fernández, J. M. Zamaro, *J. Colloid Interface Sci.*, 2014, **424**, 37-43.

24 a) X. F. Zhang, Y. G. Liu, L. Y. Kong, H. O. Liu, J. S. Qiu, W. Han, L. T. Weng, K. L. Yeung, W. D. Zhu, *J. Mater. Chem. A*, 2013, **1**, 10635-10638. b) X. F. Zhang, Y. G. Liu, S. H. Li, L. Y. Kong, H. O. Liu, Y. S. Li, W. Han, K. L. Yeung, W. D. Zhu, W. S. Yang, J. S. Qiu, *Chem. Mater.*, 2014, **26**, 1975-1981. c) D. Fairen-Jimenez, S. A. Moggach, M. T. Wharmby, P. A. Wright, S. Parsons, T. Duren, *J. Am. Chem. Soc.*, 2011, **133**, 8900-8902. d) G. Kumari, K. Jayaramulu, T. K. Maji, C. Narayana, *J. Phys. Chem. A*, 2013, **117**, 11006-11012. e) C. H. Kuo, Y. Tang, L. Y. Chou, B. T. Sneed, C. N. Brodsky, Z. Zhao, C. K. Tsung, *J. Am. Chem. Soc.*, 2012, **134**, 14345-14348.

25 a) N. E. Tsakoumis, M. Rønning, Ø. Borg, E. Rytteret, A. Holmen, *Catal. Today*, 2010, **154**, 162-182. b) G. H. Yang, D. Wang, Y. Yoneyama, Y. S. Tan, N. Tsubaki, *Chem. Commun.*, 2010, **48**, 1263-1265. c) G. H. Yang, J. J. He, Y. Yoneyama, Y. S. Tan, Y. Z. Han, N. Tsubaki, *Appl. Catal. A*, 2007, **329**, 99-105.

26 A. S. Bambal, V. S. Guggilla, E. L. Kugler, T. H. Gardneret, D. B. Dadyburjor, *Ind. Eng. Chem. Res.*, 2014, **53**, 5846-5857.